Proc. of the 8th International Conference NEET 2013, Zakopane, Poland, June 18–21, 2013

Light Emitting Single-Crystalline Silicon Wafers Implanted with V and III Group Ions

F. Komarov[a], L. Vlasukova[a], O. Milchanin[a], M. Greben[a,*], I. Parkhomenko[a], A. Mudryi[b], E. Wendler[c] and P. Zukowski[d]

[a]Belarusian State University, Nezavisimosti ave. 4, 220030 Minsk, Belarus

[b]Scientific and Practical Materials Research Center, National Academy of Sciences of Belarus P. Brovki Str. 17, 220072 Minsk, Belarus

[c]Institut für Festkörperphysik, Friedrich-Schiller-Universität Jena, Max-Wien-Platz 1, D-07743 Jena, Germany

[d]Lublin University of Technology, Nadbystrzycka 38d, 20-618 Lublin, Poland

Compound semiconductor nanocrystals (InAs, InSb, GaSb) were successfully synthesized in single crystalline Si by high fluence ion implantation at 500 °C followed by high-temperature rapid thermal annealing or conventional furnace annealing at 900–1100 °C. Rutherford backscattering spectrometry, transmission electron microscopy/transmission electron diffraction, Raman scattering, and photoluminescence were employed to characterize the implanted layers. Two different types of the broad band emission extending over 0.75–1.1 eV were observed in photoluminescence spectra of annealed samples. One of the bands disappears in photoluminescence spectra of samples annealed at 1100 °C unlike the other one.

DOI: 10.12693/APhysPolA.125.1288

PACS: 61.80.−x, 61.72.Ff, 63.20.−e, 78.66.−w

1. Introduction

A new class of structures — quantum dots (QDs) — has attracted great interest during the last two decades as they combine the advantages of bulk semiconductors with those of isolated atoms. Downsizing of electronic devices made the research of synthesis of self-assembled QDs directly in Si very promising. Because of confinement, it was expected that electrons in direct band gap QDs could occupy discrete energy levels, in a similar way as they do in atoms [1]. However, on moving from a bulk system to a dot system there arise several physical factors which control whether the interband transitions in a quantum dot will be direct or indirect. The first factor is quantum confinement effect which drives electron levels up and holes levels down in energy. The second factor is mechanical strains which can drive levels either up or down in energy. Moreover, the band alignment between QDs and surrounding matrix has to be kept in account. Finally, structural defects like dislocations that usually formed around the QDs in strained host matrix [2] could be more favorable for carrier recombination in comparison with band-to-band recombination inside QDs. Now it is already known that band line-ups of InAs/Si, InSb/Si and GaSb/Si are expected to be of type-II as indirect Si valleys lying lower in energy as a result of the upward energy shift and widening of the direct band-gap of A^3B^5 QDs due to compressive stress [3–5]. Therefore, the radiative recombination in such systems is expected to be indirect both in real- and in k-spaces [4].

In spite of it, these materials have gained significant technological interest in recent years due to their potential applications in mid-infrared optoelectronic devices. It was registered a broad band emission in the range of 0.75–1.1 eV in photoluminescence (PL) spectra of Si samples with embedded A^3B^5 nanocrystals (NCs) created by MBE [3, 4] or by ion implantation [6–9].

In this paper we report on the direct formation of A^3B^5 NCs in crystalline silicon by ion implantation followed by thermal treatment. The advantage of ion implantation technique is the areal and depth selectivity of phase formation in a substrate as well as its compatibility with industrial device production lines.

The aim of this work is to present our results on structural and optical characterization of "Si + A^3B^5 nanocrystals" system and discuss the effect of structural properties on efficiency and spectral peculiarities of photoluminescence.

2. Experimental

The specimens used for this study were prepared from lightly doped single crystalline n-type (100) Czochralski-grown silicon wafers with a resistivity of 4.5 Ω/cm. The samples were implanted at 500 °C with V and III group ions in order to create supersaturated solution of implanted species in silicon. Subsequent annealing was used to restore crystalline structure of silicon matrix as well as to synthesize compound semiconductor A^3B^5 phase in Si samples.

We performed three types of experiments differing in ion species.

In the first experiment Si samples were implanted firstly with As (170 keV, 3.2×10^{16} cm^{-2}) and then with In (250 keV, 2.8×10^{16} cm^{-2}) ions and subsequently annealed at 1050 °C for 3 min in inert ambient.

*corresponding author; e-mail: leibnits@gmail.com

In the second experiment Si samples were implanted firstly with Sb (350 keV) and then with In (350 keV) or Ga (250 keV) ions. The fluencies were 3.5×10^{16} cm^{-2} or 5×10^{16} cm^{-2} for both ion species in the case of (Sb + In) or (Sb + Ga) ion implantations, accordingly. Subsequently, implanted samples were annealed at 900–1100 °C for 30 s–60 min in Ar ambient. The samples from the first two experiments were cooled to room temperature between implantation of different ions.

In the third experiment Si samples were implanted with Ga (250 keV, 3.5×10^{16} cm^{-2}) and Sb (350 keV, 3.5×10^{16} cm^{-2}) ions. The samples were stored in a chamber with constant temperature $T = 500$ °C between implantation of different ions. Afterwards, the samples were annealed at 1100 °C for 3, 30, and 60 min in Ar ambient.

The structural properties of the samples were investigated using the Rutherford backscattering spectrometry (RBS) and transmission electron microscopy (TEM) and diffraction (TED). The RBS spectra were collected with a collimated 1.3–1.5 MeV He^+ beam at a backscattering angle of 170°. TEM experiments were performed in plan-view geometry using a Hitachi H-800 instrument operating at 200 keV. The optical properties of samples were investigated by the Raman spectroscopy and low temperature PL spectroscopy. The Raman scattering (RS) spectra were recorded at room temperature in the backscattering geometry in the range from 90 to 600 cm^{-1} using a micro-Raman setup Nanofinder with excitation wavelength of 473 nm. The PL spectra were recorded in the spectral region of 0.7–2 eV using 600 mm grating monochromator in combination with a cooled to liquid nitrogen temperature InGaAs detector. During measurements the samples were immersed in a liquid helium cryostat and the 514.5 nm line of an argon ion laser was used to excite PL.

3. Results and discussion

Figure 1a shows the depth profiles of Ga and Sb atoms in Si samples simulated stopping and ranges of ions in matter(SRIM) and calculated from the experimental RBS spectra. These calculations do not take into account the implantation temperature. Therefore, the simulated results are close to experimental depth profiles of implanted species for room temperature implantation [10] only. The depth profiles were calculated from RBS spectra by fitting of the spectra using HEAD code until the simulated spectra coincided completely with the experimental spectra.

From Fig. 1a one can see that implantation at 500 °C already leads to strong broadening and significant reduction of the impurity concentration as compared to the SRIM calculation that could be explained by transient enhanced diffusion (TED). Figure 1b presents the RBS spectra of the (Sb + In) implanted samples. One can see that high temperature annealing leads to further redistribution of impurity.

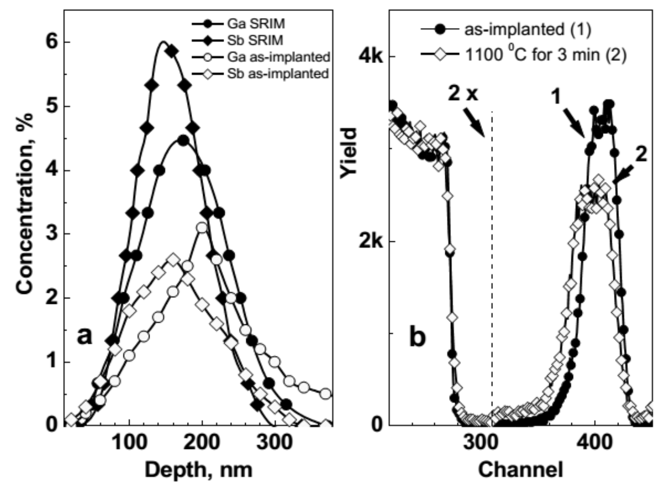

Fig. 1. Simulated (SRIM) and calculated from the RBS spectra (a) depth profiles of impurities in Si implanted with Ga (250 keV, 3.5×10^{16} cm^{-2}) and Sb (350 keV, 3.5×10^{16} cm^{-2}) ions. RBS spectra (b) of Si samples implanted (1) with Sb (350 keV, 3.5×10^{16} cm^{-2}) and In (350 keV, 3.5×10^{16} cm^{-2}) ions and annealed at 1100 °C for 3 min (2).

The results of the TEM studies in plan-view mode are depicted in Fig. 2. One can observe faceted InAs, InSb and GaSb nanoprecipitates in Si samples, implanted with (As + In), (Sb + In) and (Ga + Sb) ions, correspondingly. The crystalline nature and stoichiometry of InAs precipitates is proved by the presence of the Moire fringe patterns in the TEM images (inset in Fig. 2a) [7].

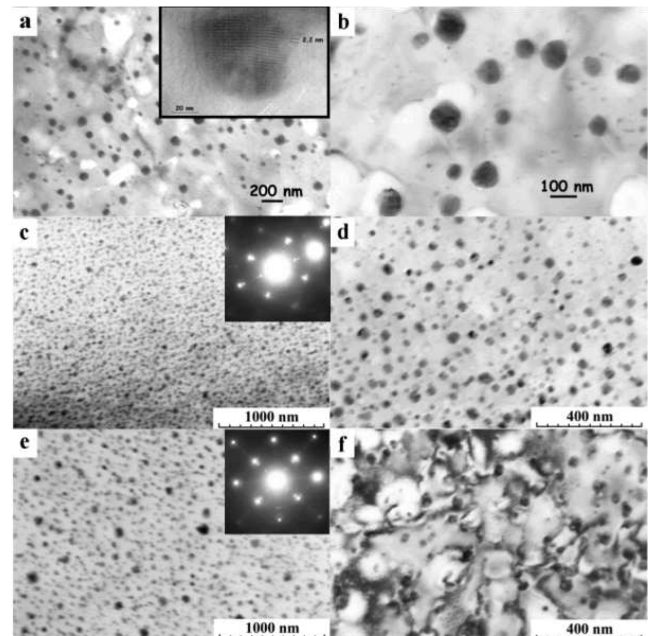

Fig. 2. Bright-field TEM images from Si samples after "hot" implantation of (As + In) (a), (b), (Sb + In) (c), (d), (Ga + Sb) (e), (f) ions and annealing at 1050 °C for 3 min (a), (b) or 1100 °C for 30 min (c), (f).

The presence of crystalline InSb and GaSb nanoprecipitates in annealed samples is proved by RS spectra (Fig. 3). Thus, a layer with A^3B^5 crystallites is formed in the annealed samples. This layer is characterized by a good structural quality in the case of (As + In) implanted samples in contrast to heavily damaged layer of samples implanted with (Sb + In) or (Ga + Sb) ions. The surface layer with InSb or GaSb nanocrystals contains a lot of dislocation loops (Fig. 2f) and microtwins (inset in Fig. 2c,e). And indeed, we failed to get aligned RBS spectra of the (Ga + Sb) implanted and annealed sample while the aligned yield almost reach the random level (not shown) in the case of (Sb + In) sample. It indicates that the layer with InSb or GaSb nanocrystals is in near amorphous state even after 1100 °C annealing.

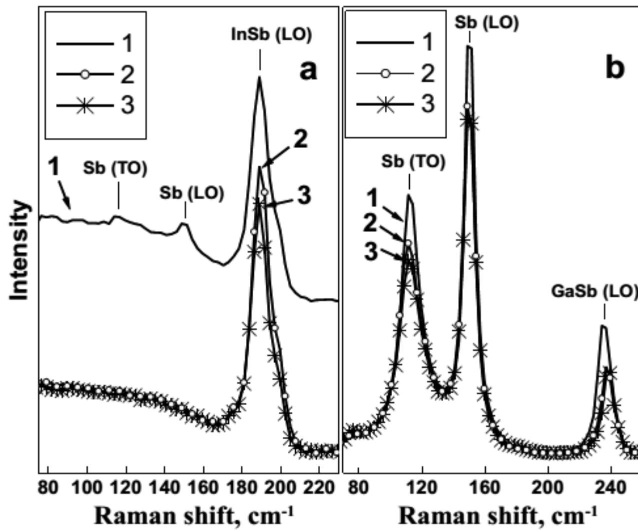

Fig. 3. RS spectra of Si samples implanted with (Sb + In) (a) or (Ga + Sb) (b) ions and annealed at 1100 °C for 3 (1), 30 (2) or 60 (3) min.

In order to identify nanocrystals RS was used. Figure 3 depicts RS spectra of implanted with (Sb + In) and (Ga + Sb) ions and annealed samples. The peaks at 189 cm^{-1} (Fig. 3a) and 235–237 cm^{-1} (Fig. 3b) should be attributed to LO-phonon scattering of crystalline InSb and GaSb, accordingly. It confirms the formation of InSb or GaSb nanocrystals in implanted layers of Si samples. Besides them, additional peaks at 115 cm^{-1} and 150 cm^{-1} present in RS spectrum (Fig. 3a) of the sample implanted with (Sb + In) ions and annealed at 1100 °C for 3 min. These peaks are the characteristic lines for crystalline Sb. For bulk Sb the frequencies of TO- and LO-phonons are 113 and 152 cm^{-1} [11], respectively. An increase of annealing duration up to 30–60 min results in disappearing of Sb lines. It indicates that Sb precipitates are present in (Sb + In) ion implanted sample after rapid thermal annealing (RTA) only. At the same time the characteristic bands for crystalline Sb are present in RS spectra of (Ga + Sb) implanted sample even after long time annealing at 1100 °C (Fig. 3b).

In addition, a narrow peak at 518 cm^{-1} corresponding to zone-center phonons scattering of crystalline silicon is registered in RS spectra (not shown) of all discussed samples. The presence of this peak confirms the crystalline state of the silicon matrix. However, it should be noted that a significant shift towards low frequencies occurs in comparison with the peak's position at 521 cm^{-1} of undamaged Si [8]. This shift is caused by the presence of significant mechanical strains within the implanted layer [8].

Figure 4 depicts the PL spectra of implanted samples. The sharp lines at 1.09 eV and 1.15 eV are related to bound exciton phononless and phonon assisted recombination at main residual doping impurity (phosphorus) or implanted donor impurity (arsenic or antimony). Besides them, the broad band emission in the range of 0.8–1.1 eV dominates in the most of PL spectra. We could distinguish two types of the broad band depending on the type of implanted species. The band presented in PL spectra of samples implanted with (As (Sb) + In) ions are observable even after annealing at 1100 °C for 60 min (Fig. 4b) and could be fitted as a superposition of at least two bands with maxima at 0.95 eV and 0.99 eV. It has been previously reported on the observation of similar broad band in PL spectra of Si samples implanted with As (Sb) and In ions and annealed by flash lamp annealing (FLA) [9], RTA [6] or conventional furnace annealing (FA) [7] at 900–1150 °C.

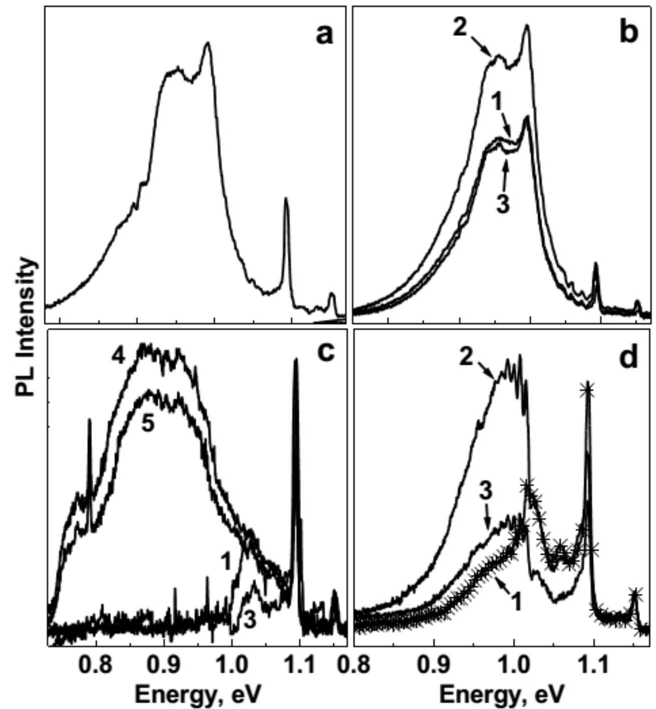

Fig. 4. PL spectra of Si samples implanted with (As + In) (a), (Sb + In) (b), (Sb + Ga) (c) or (Ga + Sb) (d) ions and annealed at 900 (4, 5), 1050 (a) or 1100 °C (1–3) for 30 s (4), 3 min (a, 1), 30 min (2), 45 min (5) or 60 min (3).

Moreover, a similar band was detected in the PL spectra of silicon samples with embedded InAs or InSb nanocrystals that were grown on Si(100) by solid-source MBE and annealed at 400 °C [4]. It has been presumed [4] that radiative recombination of localized electrons at the inhomogeneous interfaces between InAs (InSb) and Si with quantum confined holes are responsible for the band appearance in PL spectra. The question about the nature of discussed band is still open and needs further investigations. At the same time the broad band with maximum near 0.9 eV is registered in PL spectra of (Sb + Ga) ion implanted samples (Fig. 4c).

A similar band was observed earlier in the PL spectra of silicon samples with embedded tin (α-Sn) QDs in Ref. [12]. Sn QDs were formed in Si(100) as result of heat treatment up to 800 °C of a few nanometer thick Sn_xSi_{1-x} layers with $x \leq 0.1$ grown on Si surface. The appearance of this band was attributed to the presence of defects introduced by the grown layers.

In the experiment under consideration here, the similar band is registered in PL spectra of Si implanted with Sb and Ga ions. Thus, the question about the nature of this band arises. There are at least three possible explanations of near-IR photoluminescence origin for "Si + SbGa nanocrystals". They are: carrier recombination inside GaSb NCs, radiative recombination at the nanocrystal/Si matrix interfaces and dislocation-related luminescence [13]. After the annealing at 1100 °C the band at 0.75–1.1 eV disappears in the PL spectra (Fig. 4c). At the same time the PL spectra of Si/GaSb samples annealed at 1100 °C exhibit a series of relatively more sharp lines at successive line spacing of 8 meV (Fig. 4d). The spectrum transformations could be related to annealing of a part of dislocation-type defects and is presently under study by our team.

4. Conclusions

We have investigated structural and optical properties of silicon layers with embedded InAs, InSb and GaSb nanocrystals formed by high fluence ion implantation at 500 °C followed by thermal treatment at (900–1100 °C) for 30 s–1 h. A significant loss and redistributions of implanted species has been revealed by RBS experiment as a result of "hot" implantation conditions and post-implantation annealing. The formation of A^3B^5 nanocrystals in implanted Si layer was registered in all annealed samples using TEM and RS experiments. InAs NCs are formed in the Si near-surface layer of good structural quality, while the heavily damaged Si layer with InSb and GaSb NCs contains a lot of dislocation loops and microtwins. Besides A^3B^5 NCs, the Sb nanocrystals were registered in Si samples implanted with (Sb + In) or (Ga + Sb) ions and annealed at 1100 °C for 3–60 min.

Two different types of the broad bands in the range of 0.75–1.1 eV were detected in PL spectra of annealed samples. The first band was registered in PL spectra of Si samples implanted with (As (Sb) + In) ions and could be fitted as a superposition of at least two bands with maxima at 0.95 eV and 0.99 eV. This broad band is observable in PL spectra of samples annealed even at 1100 °C for 60 min. In contrast to it the band with maximum near 0.9 eV in PL spectra of (Sb + Ga) ion implanted samples are not visible after annealing at temperature as high as 1100 °C for 3–60 min.

References

[1] T. Mano, H. Fujioka, K. Ono, Y. Watanabe, M. Oshima, *Appl. Surf. Sci.* **130-132**, 760 (1998).

[2] Y.-K. Huang, C.-P. Liu, Y.-L. Lai, C.-Y. Wang, Y.-F. Lai, H.-C. Chung, *Appl. Phys. Lett.* **91**, 091921 (2007).

[3] R. Heitz, N.N. Ledentsov, D. Bimberg, A.Yu. Egorov, M.V. Maximov, V.M. Ustinov, A.E. Zhukov, Zh.I. Alferov, G.E. Cirlin, I.P. Soshnikov, N.D. Zakharov, P. Werner, U. Gosele, *Physica E* **7**, 317 (2000).

[4] M. Jo, K. Ishida, K. Kawamoto, S. Fukatsu, *Phys. Status Solidi C* **0**, 1117 (2003).

[5] S. Prucnal, S. Facsko, C. Baumgart, H. Schmidt, M.O. Liedke, L. Rebohle, A. Shalimov, H. Reuther, A. Kanjilal, A. Mucklich, M. Helm, J. Zuk, W. Skorupa, *Nanoletters* **11**, 2814 (2011).

[6] A.L. Tchebotareva, J.L. Brebner, S. Roorda, C.W. White, *Nucl. Instrum. Methods Phys. Res. B* **175-177**, 187 (2001).

[7] F. Komarov, L. Vlasukova, W. Wesch, A. Kamarou, O. Milchanin, S. Grechnyi, A. Mudryi, A. Ivankovich, *Nucl. Instrum. Methods Phys. Res. B* **266**, 3557 (2008).

[8] F. Komarov, L. Vlasukova, O. Milchanin, A. Mudryi, B. Dunets, W. Wesch, E. Wendler, *Phys. Status Solidi A* **209**, 148 (2012).

[9] S. Prucnal, M. Turek, A. Drozdziel, K. Pyszniak, A. Wojtowicz, S.-Q. Zhou, A. Kanjilal, A. Shalimov, W. Skorupa, J. Zuk, *Cent. Eur. J. Phys.* **9**, 338 (2011).

[10] F.F. Komarov, O.V. Milchanin, L.A. Vlasukova, W. Wesch, A.F. Komarov, A.V. Mudryi, *Bull. Russ. Acad. Sci., Phys.* **74**, 252 (2010).

[11] M. Landolt, J. Bornstein, *Series Numerical Data and Fuctional Relationships in Science and Technology*, Springer-Verlag, Berlin 1989.

[12] A. Karim, G.V. Hansson, W.-X. Ni, P.O. Holtz, M. Larsson, H.A. Atwater, *Opt. Mater.* **27**, 836 (2005).

[13] F. Komarov, L. Vlasukova, O. Milchanin, A. Mudryi, J. Zuk, K. Pyszniak, M. Kulic, *Acta Phys. Pol. A* **120**, 204 (2011).